ELSEVIER

Chemical Engineering Journal 135 (2008) 209–215

Chemical Engineering Journal

www.elsevier.com/locate/cej

A high throughput methodology for continuous preparation of monodispersed nanocrystals in microfluidic reactors

Ying Ying [a,b], Guangwen Chen [a,*], Yuchao Zhao [a,b], Shulian Li [a], Quan Yuan [a]

[a] *Dalian Institute of Chemical Physics, Chinese Academy of Sciences, 457 Zhongshan Road, Dalian 116023, China*
[b] *Graduate University of Chinese Academy of Sciences, Beijing 100049, China*

Received 8 November 2006; received in revised form 27 January 2007; accepted 1 March 2007

Abstract

T-type microchannel reactors were used to prepare monodispersed nanocrystals of barium sulfate and boehmite. The size of barium sulfate is strongly dependent on the velocity of the reactants in the channel. High velocity is beneficial for producing small particles. The concentration of reactants also affects the size. Boehmite was prepared by neutralization of $NaAlO_2$ and $Al_2(SO_4)_3$. Changing the proportion of $NaAlO_2$ and $Al_2(SO_4)_3$ will lead to different pH values which determine the phase of alumina. High efficiency of micromixing is the key factor of the purity of the alumina morphology. Na_2CO_3 was used to adjust pH at given value during aging process. Aging is indispensable for the amorphous alumina to crystallize to boehmite. Raising the age temperature would reduce the time the crystallization need. The morphology and purity were characterized by powder X-ray diffraction (XRD) and transmission electron microscopy (TEM).

Keywords: Microreactor; Microchannel; Nanoparticle; Micromixer; Barium sulfate; Boehmite

1. Introduction

The preparation of monodispersed nanocrystals is a very significant and challenging work for the nano-industry. Among all the methods of producing nanomaterials, the liquid–liquid chemosynthesis way is the most efficient and widely used one that traditionally proceeds in batch reactors [1]. In classic colloid chemistry, the particle formation will go through three stages in the liquid phase, i.e., nucleation, growth companying with Ostwald ripening, and aggregation [2]. While new ideas on particle formation from supersaturated systems develop rapidly, they are controversial [3]. This article would discuss based on the conventional theory. Primary nucleation usually dominates in reaction crystallization because of the high levels of supersaturation and the highly non-linear dependence of primary nucleation on supersaturation [4]. Often the nucleation processes are rapid compared to the rate of mixing of the reactants, the nonuniform distribution of the crystal nucleus and different residence time of growth and aggregation will occur due to the insufficient mixing in batch reactors, thus, broadening the crystal size distribution and debasing the nanomaterial's quality [5].

A microchannel reactor is a continuous flow-type reactor with the channels' characteristic dimensions under a millimeter in size [6,7]. The large area-to-volume ratio of micro reactors gives prospect of better heat and mass transfer rates compared to conventional reactors, and so it allows reactions to be performed under more severe conditions with higher yields. Certain reactions too fast to be performed in conventional reactors can be accomplished in microchannel reactors. The characteristic time of the transport processes is massively reduced and becomes comparable to that of the chemical reaction. Some mixing-controlled syntheses would then turn into reaction-controlled ones in the microchannel reactors. High efficiency of micromixing is the key factor to prepare monodispersed nanocrystals with controllable properties. Thus the traits of short transport time and high efficient micromixing make the microchannel reactors to be idea equipments to produce controllable monodispersed nanocrystals.

Lately, its application for nanoparticles production is attracting much interest. Many organizations have joined the work of using microchannel reactors to synthesize nanocrystals of semiconductors [8–15], metals [16–18], colloids [19,20], zeolite [21], organic compound [22], and catalyst [23], etc. All

* Corresponding author. Tel.: +86 411 8437 9031; fax: +86 411 8469 1570.
E-mail address: gwchen@dicp.ac.cn (G. Chen).

1385-8947/$ – see front matter © 2007 Elsevier B.V. All rights reserved.
doi:10.1016/j.cej.2007.03.009

these works demonstrated that microchannel reactors were quite suitable for continuous preparation of nanocrystals and showed great advantages in controlling reaction conditions and particle properties. However, most of the experiments proceeded at such a low velocity that the mixing is predominated almost exclusively by molecular diffusion. Furthermore, the laminar flow causes velocity profiles in the channel to appear typically parabolic in shape, which can lead to a relatively broad residence-time distribution. Many organizations introduce using slug flow with gas or insoluble liquid as separated medium [15,19,20,24–26]. This method greatly enhances the micromixing performance, but requires scrupulous operations and very low throughput for the sake of the frail stability of special flow pattern.

Here we employ T-type microchannel reactors to prepare nanocrystals with high throughput [27,28]. The T-type microchannel reactor provides a vortex chamber at the T-junction. With high flow velocity, the impinging of the two reactants at the T-junction leads to chaotic flow [29–31]. The turbulence provides an efficient micromixing of the reactants, which is beneficial for preparing monodispersed nanocrystals. Moreover, with minimal amounts of reagents, we can use microfluidic reactors to find out the optimal parameters for the monodispersed nanocrystals preparation in a short time.

2. Experimental section

2.1. Structure of the reactor

The reacting system and the sketch of the channels are showed in Fig. 1. The microchannels are fabricated in a polymethyl methacrylate (PMMA) substrate using micromachining technology. There are two feed channels positioned horizontally opposite each other and a vertical one meeting them at the crunode, where the reactants impinge and flow through the vertical channel as the reaction proceeds. The channel-board is covered on a blank substrate and tightened with screws. Sketch of the channels: Reactor 1 has the inlet channels with the dimension of 0.2 (width) × 0.2 (depth) × 10 (length) mm, and the reaction channel of 1 mm × 0.2 mm × 20 mm. Reactor 2 has the inlet channels of 1 mm × 1 mm × 20 mm, and the reaction channel of 1 mm × 1 mm × 40 mm.

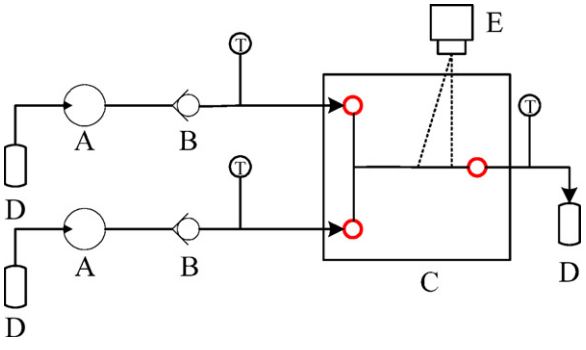

Fig. 1. Schematic diagram of experimental set-up: A, pump; B, check valve; C, T-type microchannel reactor; D, tank; E, CCD camera.

2.2. Villermaux–Dushman system

The Villermaux–Dushman system is a reaction between iodide and iodate coupled with a neutralization reaction [32]. It is a widely used parallel competing reaction system to quantify the micromixing quality in an explicit way. The reaction formulas are shown as follows:

$$H_2BO_3^- + H^+ \rightarrow H_3BO_3 \quad \text{quasi-instantaneous,} \tag{1}$$

$$5I^- + IO_3^- + 6H^+ \rightarrow 3I_2 + 3H_2O \quad \text{very fast,} \tag{2}$$

$$I_2 + I^- \rightleftharpoons I_3^- \quad \text{quasi-instantaneous.} \tag{3}$$

The redox reaction (2) is fast, in the same range of the micromixing process, but is much slower than the neutralization reaction (1). In perfect mixing conditions, the injected acid is instantaneously dispersed in the reactive medium and consumed by borate ions according to reaction (1). While the micromixing time is in the same range or larger than the characteristic reaction time of reaction (2), these aggregates involve extra acid can react with iodide and iodate surrounding ions to yield iodine. The iodine can further react with iodide ions I^- to yield I_3^- ions according to reaction (3). I_3^- concentration can be easily measured by spectrophotometry at 353 nm.

Segregation index X_s is used to express the micromixing in an explicit way. In perfect micromixing conditions the X_s is 0, while in total segregation X_s is 1. X_s is defined as [32]:

$$X_s = \frac{Y}{Y_{ST}}, \tag{4}$$

with

$$Y = \frac{2(n_{I_2} + n_{I_3^-})}{n_{(H^+)_0}} = \frac{2V_{total}([I_2] + [I_3^-])}{V_{acid}[H^+]_0}, \tag{5}$$

$$Y_{ST} = \frac{6[IO_3^-]_0/[H_2BO_3^-]_0}{6([IO_3^-]_0/[H_2BO_3^-]_0) + 1}. \tag{6}$$

Here, Y is the ratio of acid mole number consumed by reaction (2) divided by the total acid mole number and Y_{ST} is the value of Y in total segregation case. V_{acid} is volumetric flow rate of acid, V_{total} is total volumetric flow rate of acid and mixed solution of H_3BO_3, NaOH, KI and KIO_3.

2.3. Materials and methods

Na_2SO_4 (Shenyang federation reagent factory, analytic grade) and $BaCl_2{\cdot}2H_2O$ (Shenyang xingshun chemical reagent factory, analytic grade) were dissolved separately in distilled water with no further purification. The two solutions were pumped into Reactor 1 through two inlets respectively. The pumps and reactor are connected by PVC pipes with diameters of 3 mm. Two pumps were set at the same flow rate. The nanocrystals were collected by beakers at the outlet. As to the direct chemical precipitation way, $BaCl_2$ solution was added into Na_2SO_4 solution dropwise under high-speed magnetic stirring condition.

$NaAlO_2$ (Guoyao group chemical reagent company, analytic grade) and $Al_2(SO_4)_3{\cdot}18H_2O$ (Shenyang third reagent factory, analytic grade) were dissolved in water. The concentrations of $NaAlO_2$ and $Al_2(SO_4)_3$ were 0.6 and 0.1 mol/L, respectively. The solutions must be used within 8 h since the $NaAlO_2$ are tending to hydrolyze to $Al(OH)_3$. The precursors were pumped into Reactor 2 at various flux controlled by two pumps separately. The flow rates of $Al_2(SO_4)_3$ were set at 9 mL/min while the flow rates of $NaAlO_2$ were varied between 4.2 and 6.0 mL/min according to the pH value. The reactor and a part of pipes were dipped into a water bath for temperature control. The products collected at the outlet by beakers were then aged for a certain time. During the aging time, the beaker was dipped in the water bath for temperature control. Na_2CO_3 (Shenyang federation reagent factory, analytic grade) was added if the pH value needed to be increased during the aging process. It was then washed three times by distilled water in a centrifugal machine and dried in an oven at 110 °C.

The structure characterization of boehmite was carried out by powder X-ray diffraction (Rigaku Japan) in a 2θ range from 5° to 70° with a Cu Kα radiation operating at 30 kV and 15 mA. The morphologies of the nanoparticles were observed by transmission electron microscopy (TEM, JEOL) images.

3. Results and discussion

3.1. Micromixing in the microchannel reactor

The efficiency of micromixing of the T-type reactor has been investigated in our group using Villermaux–Dushman parallel competing reactions and CCD camera [33]. H_2SO_4 was diluted to 1.8×10^{-2} mol/L. The mixed solution of H_3BO_3, NaOH, KI and KIO_3, with the concentration of 0.25, 0.125, 0.0116, 0.00233 mol/L respectively was prepared. CCD camera was fixed at the reaction channel near the outlet, where fluids were full developed. At low *Re* number, micromixing quality gets better as flow rate increases. When the flux is high enough, X_s is close to 5.0×10^{-4}, suggesting almost perfect micromixing. The mixing flow patterns with two dyed water were observed via CCD camera. Fig. 2(b) shows that nearly perfect micromixing is achieved at high *Re* number.

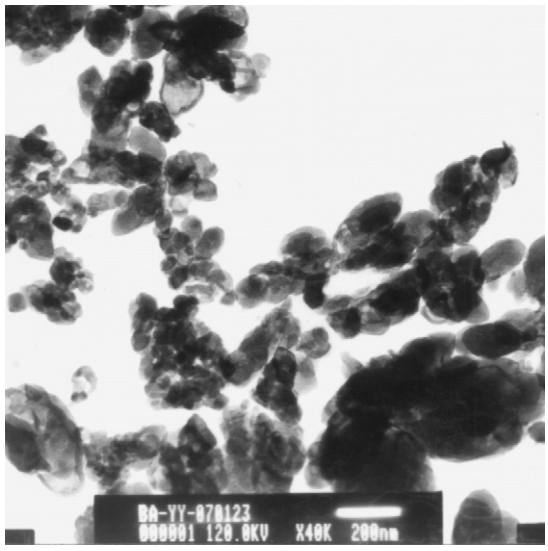

Fig. 3. TEM image of $BaSO_4$ prepared by direct precipitation.

3.2. $BaSO_4$ synthesis

3.2.1. Direct precipitation way

Fig. 3 shows the TEM image of $BaSO_4$ prepared by direct precipitation way in a beaker. The concentrations of both reactants were 0.5 mol/L. The precipitation process goes through three steps in the liquids, nucleation, crystal growth and aggregation. All the steps finished in a short time. And the process is a mixing-sensitive one. In a beaker, the mixing environment is various, and the mixing intense is not strong enough to mix the reactants in a molecular scale before reaction. It's difficult to produce monodispersed nanoparticles in a beaker.

3.2.2. Microchannel way

Reactor 1 was employed for $BaSO_4$ synthesis. Fig. 4 shows the TEM images of the samples produced by the microchannel reactor. All the samples are smaller and obtain a much even size distribution than the ones in Fig. 3. The micromixing environment in the microchannels is much better than in the conventional beakers. The pumps were limited to a certain volume rate of 20 mL/min. And the inlet channels were designed much narrower to accelerate the velocity. The impinging of

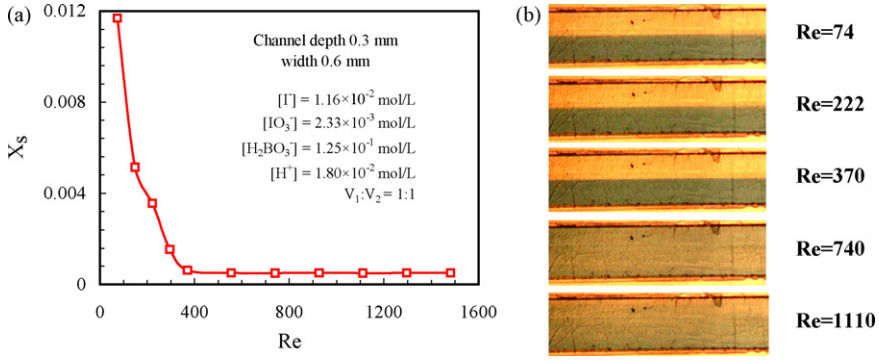

Fig. 2. (a) X_s vs. *Re* number; (b) CCD images of two liquids mixing at different *Re* number. The flow was from the left to the right.

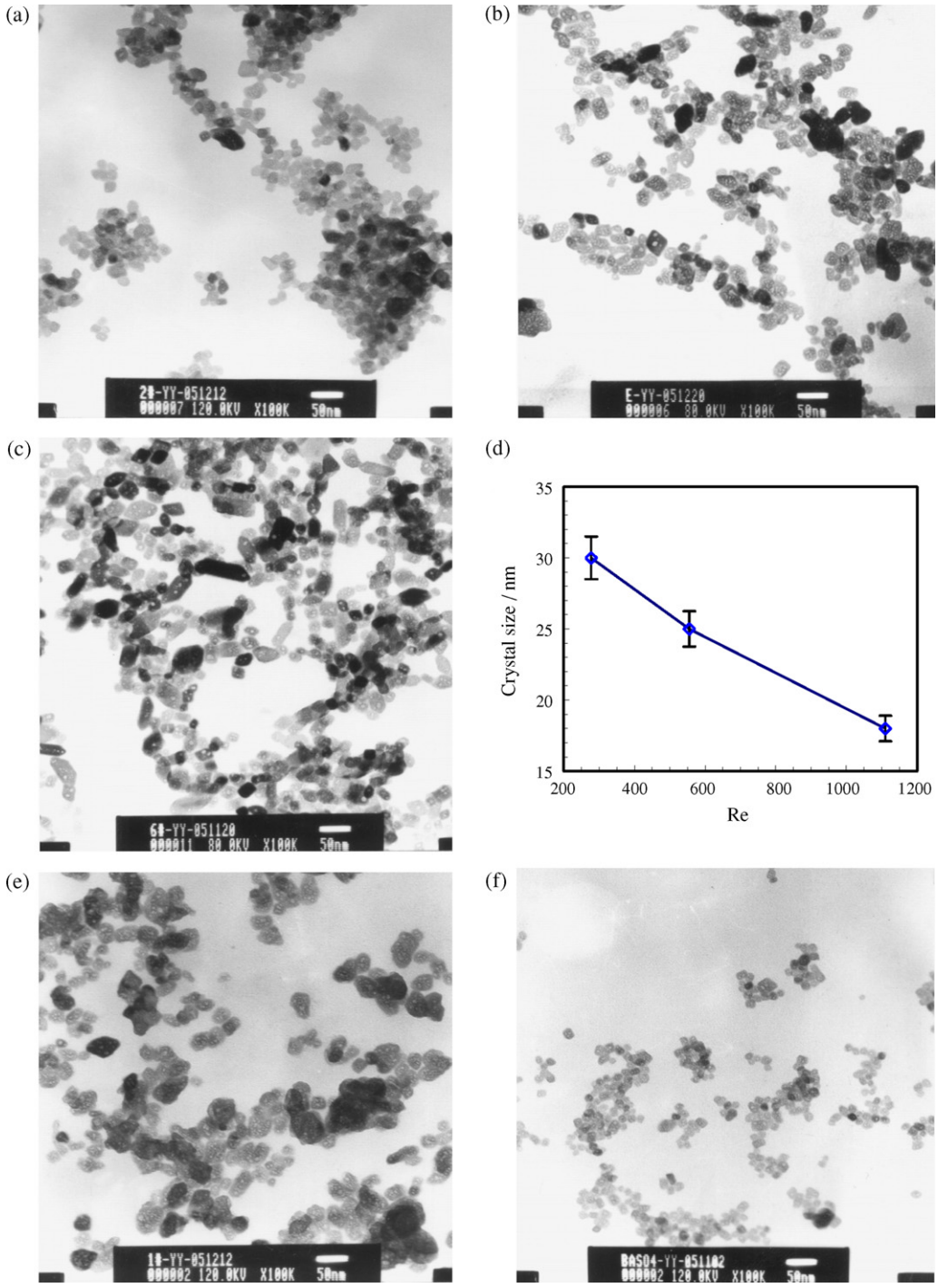

Fig. 4. (a–c, e, f) TEM images of $BaSO_4$ crystals; (d) crystal size vs. *Re* number. Flow rate (mL/min): (a, e, f) 20; (b) 10; (c) 5.0. Concentration (mol/L): (a, b, c) 0.5; (e) 0.1; (f) 10.

liquids with high velocities at the T-junction induced high intensity of vortex which led to efficient micromixing.

Flow rates have great influence on the micromixing in the channels. Na_2SO_4 and $BaCl_2$ under different flow rates of 20, 10 and 5 mL/min were applied to synthesize $BaSO_4$. The highest velocity at the inlet channels were 8.33 m/s, and reached relative velocity of 16.7 m/s at the impinging crunode. The *Re* numbers at the reaction channel were about 1110, 555 and 278 at different flow rates, respectively.

The TEM images of Fig. 4 show that the crystal size is small and narrowly distributed at high throughput of 40 mL/min of $BaSO_4$. The size is about 18 nm when the *Re* is around 1110. As the throughput reduced, the nanocrystals get larger and uneven due to the insufficient micromixing. It shows that better micromixing does help to improve monodispersed nanocrystals.

Effects of different concentrations were studied when the flow rates were set at 20 mL/min as a constant. The particles are near 18 nm and uniform when the concentration is 0.5 mol/L

Table 1
Preparation conditions and properties of samples tested by XRD

Sample	Precipitation pH	Aging pH	Aging time (h)	Reaction temperature (°C)	Aging temperature (°C)	*d*-Value of (0 2 0) plane (nm)	Structure
1	6	6	2	25	45	–	Amorphous
2	7	7	2	45	45	–	Amorphous
3	6	8	2	25	45	0.65436	Boehmite
4	7	8.5	2	45	45	0.60372	Boehmite
5	8	8	2	45	45	0.61457	Boehmite
6	7.5	9	2	25	45	0.63656	Boehmite
7	9	9	11	45	25	–	Bayerite
8	7.5	7.5	4	25	25	–	Amorphous
9	7	8	24	25	25	0.65340	Boehmite
10	7	8	2	25	45	0.64207	Boehmite
11	7	8	17.5	25	45	0.63474	Boehmite
12	7.5	9	24	25	45	0.63203	Boehmite
13	8.5	9.5	4	25	45	0.63203	Boehmite
14	8.5	8.5	23	25	45	0.63656	Boehmite
Com[a]	–	–	–	–	–	0.60619	Boehmite

[a] Commercial sample.

as showed in Fig. 4(a). When reduced it to 0.1 mol/L, as showing in Fig. 4(e), the particles grew to above 20 nm. Some of them even reached to 25 nm. This would attribute to the relatively small number of nuclei at low concentration. Thus the molecules that each nucleus could get abundant. Particles grew larger by absorbing numerous $BaSO_4$ molecules in the liquid. When increase it to 1.0 mol/L, the smallest particles reach to 12 nm, however the uniformity gets slightly worse. The influence of concentration suggests the importance of the nucleation stage.

3.3. Boehmite neutralization

Reactor 2 was used for boehmite synthesis. It is widely known that certain preparation parameters, like pH values and aging conditions, strongly affect the structure of the alumina obtained [34–36]. The influence of parameters on the structure of boehmite is investigated using the T-type microchannel reactor. Table 1 lists the preparation conditions and various properties of the samples. The properties of a commercial sample were also tested for comparison.

The structure of alumina strongly depends on pH values. The pH values of the precipitation process were measured at the outlet. When the pH value was below 6, the outlet liquid was translucent and no precipitation was observed. By enlarging the velocity of $NaAlO_2$ to raise the pH value over 9, a suspension of opacity was prepared which turned out to be bayerite. To prepare boehmite, the outlet pH values should be between 6 and 9 when the suspension is translucent gel-like. The pH value during the aging process is also critical to prepare boehmite. It needs to be over 8. Otherwise, the gel-like products would remain amorphous. Fig. 5 shows the regions of pH values for different alumina morphologies after aging for a sufficient time.

Fig. 6 shows the XRD results of samples prepared at different pH values. The influence of pH values on the structure of the products may comes from the difference in solubility of alumina at solutions with different pH values [37,38]. At low aging pH

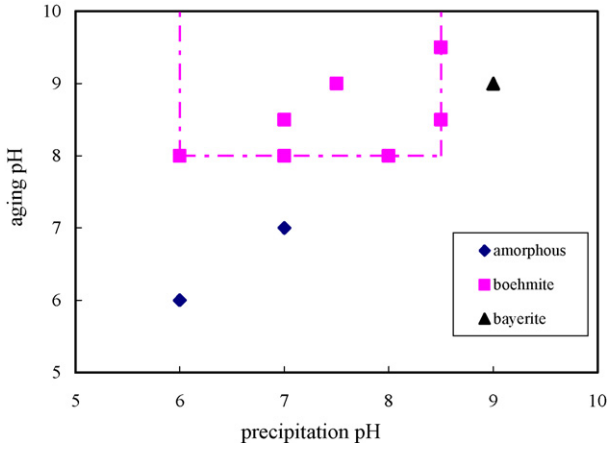

Fig. 5. Field map of products of different alumina structure prepared at varied pH values (exclusive of sample 8). The region inside dashed lines is suitable for producing boehmite.

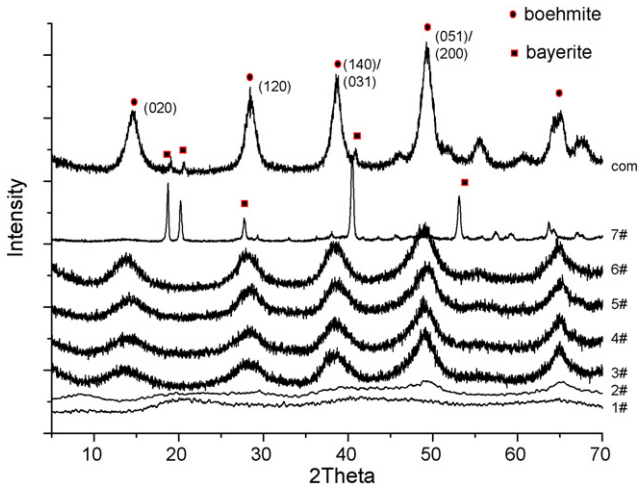

Fig. 6. XRD patterns of samples prepared at different pH value.

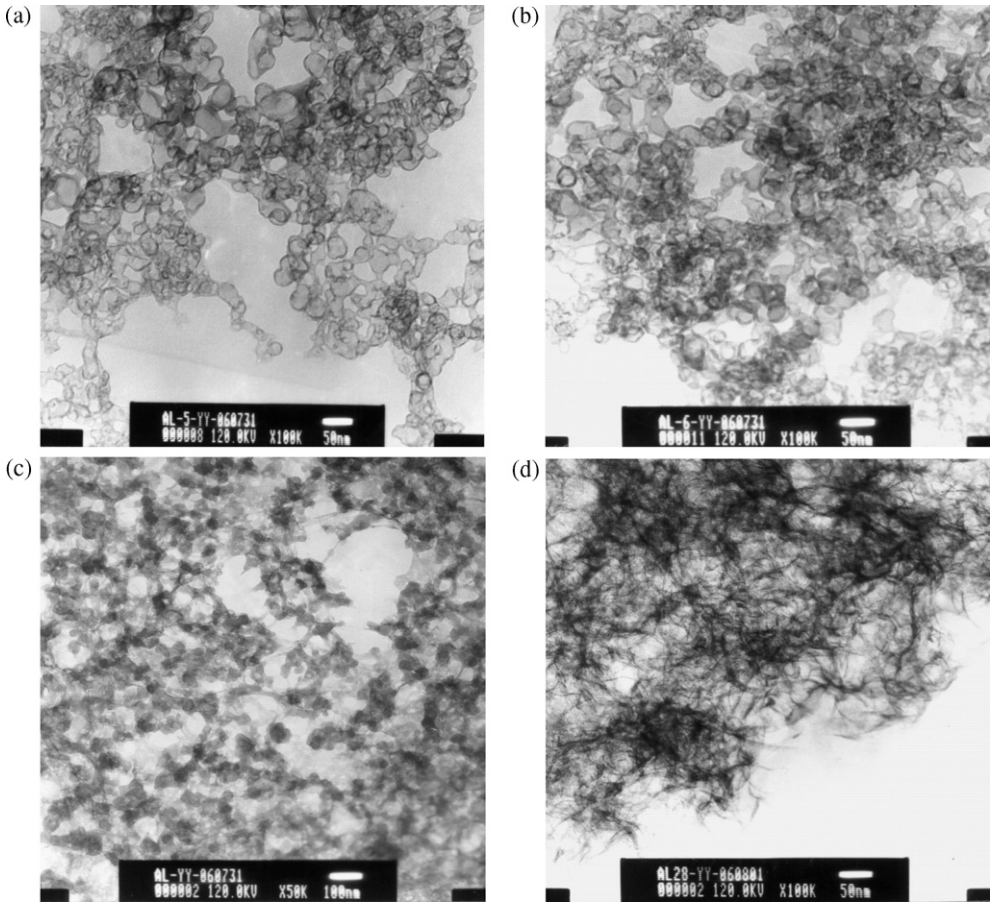

Fig. 7. TEM images of samples prepared on different aging conditions: (a) sample 9 without aging; (b) sample 1 aging at 45 °C for 2 h at acidic environment; (c) sample 10 aging for 2 h at 45 °C at alkaline environment; (d) sample 11 aging for 17.5 h at 45 °C at alkaline environment.

value (<8.0), the products could not crystallize spontaneously. The XRD patterns possess no obvious peaks and relatively low intensity, which indicate amorphous behavior as samples 1 and 2 show. When Na_2CO_3 was added during the aging process to elevate the pH value to above 8.0, the dissolution-reprecipitation process would go forward and boehmite forms, just as what samples 3 and 4 showed. Increasing the velocity of $NaAlO_2$ to raise the pH value to above 8.0, the boehmite would crystallize whether Na_2CO_3 was added or not. When the pH value becomes too high, the bayerite would form instead of boehmite as indicated in the test of sample 7.

The pH value during the precipitation process also affects the structure. The molar ratio of $NaAlO_2$ and $Al_2(SO_4)_3$ must be exactly controlled. In conventional batch process, the proportions are varied throughout the reactor due to its poor micromixing. As a result, the product is a mixture of alumina with different structures. The commercial sample contains peaks with 19° and 21° ascribed to bayerite. Microchannel reactor can ensure the homogeneity of the mixture of $NaAlO_2$ and $Al_2(SO_4)_3$ and hence lead to high purities of the crystal structure. The XRD data indicate that boehmite is the only crystalline alumina structure formed.

Aging is the spontaneous evolution of a gel structure which results from a reordering of its crystalline state. During aging process, the alumina would dissolve and reprecipitate as the process moves toward the equilibrium. The solubility of boehmite is a function of pH and temperature. At low temperature the dissolution–reprecipitation process is slow. After aging at 25 °C for 4 h, sample 8 remains amorphous. Increasing aging temperature to 45 °C, the product crystallized after 2 h of aging. For low temperature condition, the reordering process needs longer time.

Fig. 7 shows the images of morphology changes of the gels by TEM with varied aging conditions. Fig. 7(a) is the image of sample 9 without aging. Fig. 7(b) is the image of sample 1 after aging for 2 h at 45 °C at acidic environment. Particles with internal hollows are observed in both images. It suggests that the dissolution–reprecipitation reaction could not occur at low pHs. This phenomenon accords with the XRD results that all samples prepared at acidic environment are amorphous. Fig. 7(c) is the TEM image of sample 10 after aging for 2 h at 45 °C and the particles are much smaller and condensed. Hollows inside the particles disappear and fiber forms between the rounded particles. Prolong age time to 17.5 h at 45 °C, and the particles all transform to fiber as Fig. 7(d) shows for sample 11.

4. Conclusion

In conclusion, a simple and robust method has been successfully developed to produce controllable monodispersed

nanocrystals at high throughput. The turbulent flow caused by intense impinging with the relative velocity of 16.6 m/s at the T-junction enhances the micromixing, and results in a homogeneous reaction environment. Various $BaSO_4$ nanocrystal sizes could be obtained by simply changing the flow rate, that is, the performance of micromixing. Monodispersed $BaSO_4$ nanocrystals of 18 nm were prepared. The microchannel reactors are also suitable to be used to optimize the operating parameters since it can quickly generate results with a small consumption of reagents. The optimal parameters of pHs and aging conditions for boehmite preparation in the microchannel reactor are obtained. When the pH values were between 7 and 9, pure and well-crystallized boehmite were obtained after aging for a certain time. Continuous nanaoparticle production with high throughput in microchannel reactor is convenient for industrial production. Scale-up production by numbering-up of microchannel reactors can eliminate time-consuming pilot plant experiments, thereby shortening the development time from laboratory to commercial production.

Acknowledgements

We gratefully acknowledge the financial supports for this project from National Natural Science Foundation of China and China National Petroleum Corporation (nos. 20490208 and 20676129), 863 Program (2006AA05Z233) and Innovative Fund of Dalian Institute of Chemical Physics, Chinese Academy of Sciences (no. K2006D62).

References

[1] B.L. Cushing, V.L. Kolesnichenko, C.J. O'Connor, Chem. Rev. 104 (2004) 3893–3946.
[2] V.K. LaMer, R.H. Dinegar, J. Am. Chem. Soc. 72 (1950) 4847–4854.
[3] D. Horn, J. Rieger, Angew. Chem. Int. Ed. 40 (2001) 4330–4361.
[4] R. Zauner, A.G. Jones, Chem. Eng. Sci. 57 (2002) 821–831.
[5] N.V. Mantzaris, Chem. Eng. Sci. 60 (2005) 4749–4770.
[6] K.F. Jensen, Chem. Eng. Sci. 56 (2001) 293–303.
[7] K. Jahnisch, V. Hessel, H. Lowe, M. Baerns, Angew. Chem. Int. Ed. 43 (2004) 406–446.
[8] J. deMello, A. deMello, Lab Chip 4 (2004) 11N–15N.
[9] H. Nakamura, Y. Yamagrchi, M. Miyazaki, H. Maeda, M. Uehara, P. Mulvaney, Chem. Commun. (2002) 2844–2845.
[10] H. Nakamura, A. Tashiro, Y. Yamaguchi, M. Miyazaki, T. Watari, H. Shimizu, H. Maeda, Lab Chip 4 (2004) 237–240.
[11] H. Wang, X. Li, M. Uehara, Y. Yamaguchi, H. Nakamura, M. Miyazaki, H. Shimizu, H. Maeda, Chem. Commun. (2004) 48–49.
[12] B.K.H. Yen, N.E. Stott, K.F. Jensen, M.G. Bawendi, Adv. Mater. 15 (2003) 1858–1862.
[13] J.B. Edel, R. Fortt, J.C. deMello, A.J. deMello, Chem. Commun. (2002) 1136–1137.
[14] E.M. Chan, R.A. Mathies, A.P. Alivisatos, Nano Lett. 3 (2003) 199–201.
[15] I. Shestopalov, J.D. Tice, R.F. Ismagilov, Lab Chip 4 (2004) 316–321.
[16] X. Lin, A.D. Terepka, H. Yang, Nano Lett. 4 (2004) 2227–2232.
[17] J. Wagner, T. Kirner, G. Mayer, J. Albert, J.M. Köhler, Chem. Eng. J. 101 (2004) 251–260.
[18] J. Wagner, J.M. Köhler, Nano Lett. 5 (2005) 685–691.
[19] A. Gunther, S.A. Khan, M. Thalmann, F. Trachsel, K.F. Jensen, Lab Chip 4 (2004) 278–286.
[20] S.A. Khan, A.l Gunther, M.A. Schmidt, K.F. Jensen, Langmuir 20 (2004) 8604–8611.
[21] J. Ju, C. Zeng, L. Zhang, N. Xu, Chem. Eng. J. 116 (2006) 115–121.
[22] T. Kawaguchi, H. Miyata, K. Ataka, K. Mae, J. Yoshida, Angew. Chem. Int. Ed. 44 (2005) 2413–2416.
[23] M. Schur, B. Bems, A. Dassenoy, I. Kassatkine, J. Urban, H. Wilmes, O. Hinrichsen, M. Muhler, R. Schlogl, Angew. Chem. Int. Ed. 42 (2003) 3815–3817.
[24] B. Zheng, F. Rustem, Ismagilov, Angew. Chem. Int. Ed. 44 (2005) 2520–2523.
[25] H. Song, J.D. Tice, R.F. Ismagilov, Angew. Chem. Int. Ed. 42 (2003) 767–772.
[26] V.S. Shirure, A.S. Pore, V.G. Pangarkar, Ind. Eng. Chem. Res. 44 (2005) 5500–5507.
[27] Y. Jun, G. Chen, Q. Yuan, L. Luo, Y. Gonthier, Chem. Eng. Sci. 62 (2007) 2096–2108.
[28] Y. Zhao, G. Chen, Q. Yuan, AIChE J. 52 (2006) 4052–4060.
[29] T. Kuo, H. Kim, D.M. Cannon Jr., M.A. Shannon, J.V. Sweedler, P.W. Bohn, Angew. Chem. Int. Ed. 43 (2004) 1862–1865.
[30] D. Bothe, C. Stemich, H. Warnecke, Chem. Eng. Sci. 61 (2006) 2950–2958.
[31] H.C. Schwarzer, F. Schwarfirm, M. Manhart, H.J. Schmid, W. Peukert, Chem. Eng. Sci. 61 (2006) 167–181.
[32] P. Guichardon, L. Falk, Chem. Eng. Sci. 55 (2000) 4233–4243.
[33] Y.C. Zhao, Y. Ying, G.W. Chen, Q. Yuan, J. Chem. Ind. Eng. (China) 57 (2006) 1884–1890.
[34] B.P. Gyani, J. Phys. Chem. 56 (1952) 762–763.
[35] Y. Cesteros, P. Salagre, F. Medina, J.E. Sueiras, Chem. Mater. 11 (1999) 123–129.
[36] F.P. Faria, P.S. Santos, H.S. Santos, Mater. Chem. Phys. 76 (2002) 267–273.
[37] B.R. Baker, R.M. Pearson, J. Catal. 33 (1974) 265–278.
[38] K. Okada, T. Nagashima, Y. Kameshima, A. Yasumori, T. Tsukada, J. Colloid Interf. Sci. 253 (2002) 308–314.